

A prototype continuous-flow liquid–liquid extraction system using open-source technology†

Matthew O'Brien,^{*a,b} Peter Koos,^a Duncan L. Browne^a and Steven V. Ley^a

Received 12th May 2012, Accepted 11th July 2012

DOI: 10.1039/c2ob25912e

A prototype continuous-flow liquid–liquid extraction system is reported. By harnessing several open-source software libraries, a computer control script was written using the Python programming language. Using a 'computer-vision' approach, this allowed the computer to monitor the interface level between the organic and aqueous phases using a simple webcam setup and (by dynamically controlling pump flow rate) to keep this interface within defined limits. The system enabled the efficient 'inline' extraction of excess reagent in hydrazone formations, dithiane formations and epoxidations. The initial results of dispersion measurement are also presented.

Flow chemistry is emerging as a powerful enabling and transformational technology in chemical synthesis.¹ One of many advantages, compared with batch processing, is the potential for enhanced safety since only a small fraction of the reactants are being processed at any one time, making flow chemistry attractive for processes which involve hazardous intermediates or high temperatures and pressures. Also, as reactions are scaled over time rather than space, this leads to the scale-invariance of key factors such as residence or mixing times and interfacial mass/heat transfer (which depend heavily on surface-area to volume ratios), providing scope for greater reproducibility and control. Furthermore, the possibility of inline purification (e.g. scavenging,² phase-switching³) minimises labour intensive operations (such as chromatography) and thereby accommodates the use of excess reagent to drive reactions to completion. Solid supported reagents, which remove unwanted species by inline capture, have dominated this aspect of flow chemistry, and a wide range of supported functionalities are now available. However, while these materials remain the reagent of choice for many applications, they do have certain limitations in some circumstances. Aside from the high increased per-mole cost compared with

solution-phase equivalents,⁴ their depletion over time negates the time/scale invariance benefits of flow chemistry, especially at larger scales. Simply increasing the amount of solid-supported reagent (to allow scale-up or sequential runs) leads to unwanted and *scale-dependent* dispersion/diffusion effects. As the solid-supported reagent cannot normally be processed/recycled continuously (without complex parallel regeneration schemes) such systems cannot be operated in a truly continuous fashion. Solid supported catalysts, which do not suffer from depletion, have also been used successfully in continuous flow chemistry.⁵ Given the ease with which liquid–liquid separations are incorporated into batch laboratory processes, and the fact that liquids can easily be processed continually using pumps, this mode of separation (which is commonly employed in large scale industrial processes)⁶ has been used in surprisingly few laboratory-scale flow chemistry processes. Although systems which use selective wetting of expanded porous PTFE (and other porous materials) and related phenomena have been used to separate aqueous and organic biphasic mixtures,⁷ their operation often requires quite careful control of the pressure differential across the membrane, placing limitations on their use. Additionally, such systems do not easily allow the separation of immiscible organic liquid pairs (e.g. MeCN–hexane, fluoros–non-fluoros⁸). We sought therefore to develop a general purpose, operationally simple continuous-flow liquid–liquid extraction system that could be used with any immiscible pair of liquids. By using relatively cheap and readily available hardware, in combination with open-source software, we aimed to make the system as accessible as possible for others to use, modify and improve freely. The simplest way to separate two immiscible liquid phases with different densities is to use gravity. However,

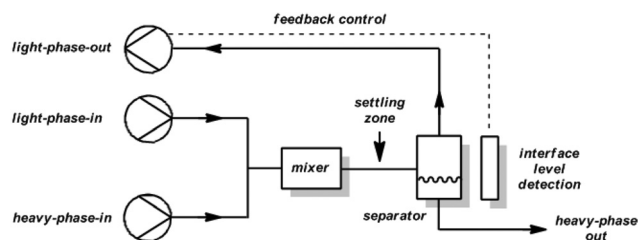


Fig. 1 Basic schematic for a continuous-flow liquid–liquid extractor.

^aWhiffen Laboratory, Department of Chemistry, University of Cambridge, Lensfield Road, Cambridge, CB21EW, UK

^bSynthetic and Medicinal Chemistry Cluster, Lennard-Jones Building, Keele University, Keele, Staffordshire, ST5 5BG, UK.
E-mail: m.o'brien@keele.ac.uk

†Electronic supplementary information (ESI) available: Technical data including software scripts and calibration data. See DOI: 10.1039/c2ob25912e

to apply this in continuous flow,⁹ several issues need to be addressed. Firstly, after mixing, the phases must separate rapidly to ensure complete partition before the point of division. Secondly, the dimensions of the gravity-separation vessel have to be sufficient to allow the phases to overcome surface forces which dominate at very small scales. This will naturally introduce a certain degree of dispersion/mixing. A significant advantage of such a system, compared with solid supported reagents, would be that, by minimising and fixing these volumes, any dispersion will be *scale-invariant*.

The ability to accurately predict and control dispersion is important for multistep continuous-flow processes where reagents for downstream reactions need to be mixed into the flow stream with matching of stoichiometry.¹⁰ The basic outline of our system, if the desired product is in the heavy phase (e.g. DCM) and the by-products/reagents are in the light phase (e.g. aqueous), is shown in Fig. 1 (the opposite configuration is of course also possible). The light and heavy phases are pumped through narrow-bore tubing, mixed together at a junction and fed into a mixer which should rapidly emulsify the two phases to enable efficient extraction. The emulsion passes into a section of narrow bore tubing, where it should instantly reform a biphasic flow stream, before passing into the separation vessel where light and heavy phases separate under gravity. A key consideration here is control of the interface position, which must remain in the separation vessel at all times. Although this could be attempted by accurately matching the flow rates of the light-phase-in and light-phase-out streams, during operation the volume of the light-phase-out may change significantly with respect to the light-phase-in as material is extracted from the heavy-phase. We aimed to use a feedback loop to the control circuitry in order to dynamically adjust the flow rate of the light-phase-out stream, keeping the interface at the desired position. This should set up a 'steady-state' for the volume of the light phase. The heavy-phase, added to this steady light-phase state, will then exit the system through the outlet at the bottom of the separation vessel *at the same rate at which it enters the separation vessel*.

We first addressed the dimensions of the separation vessel. Whilst keeping its width to a minimum would minimise mixing volume (and therefore reduce dispersion), the use of too narrow a vessel left the phases without room to settle properly. We found that a vertical cylinder with a 10 mm diameter was sufficient to facilitate separation of a segmented flow of DCM–water (and other immiscible combinations, e.g. Et₂O–water, EtOAc–water). We then turned our attention to the mixing and subsequent settling of the two phases. Rapid mixing was achieved using 4 small PTFE coated cylindrical magnets in a 4.7 mm bore tube (placed directly on a magnetic stirrer) through which the biphasic mixture was passed.¹¹ This was sufficient to emulsify a segmented flow of DCM–water in less than a second. Pleasingly, upon exiting the mixer through the narrow bore tubing at the outlet, the emulsion *immediately* separated into segmented flow again. With regard to control of the interface position, whilst it would be possible to measure some physical difference between the phases (e.g. refractive index,¹² conductivity/impedance, etc.) to detect this, we considered that direct monitoring of the interface itself would lead to far greater generality. To achieve this, we developed a 'computer-vision' system, using a cheap and

readily available web-cam to 'see' the interface. The software we wrote to accomplish this¹³ was written using the Python programming language¹⁴ and made use of several powerful open-source and freely distributed libraries including Numpy,¹⁵ OpenCV¹⁶ (computer-vision), VideoCapture¹⁷ (Python connection to Web-Cam), Python-Imaging-Library¹⁸ (Image file manipulation) and PySerial¹⁹ (Python serial communication). To simplify recognition of the interface position, we used a small ball of green plastic that had a density in-between that of the light and heavy phases (*ca.* 1 : 1 polymer melt of polyethylene and polymethoxyacetal worked well for aqueous–DCM), so that it would sit at the interface. The software allowed setting of reference points and selection of the coloured float.

During each run, several image-processing algorithms process frames sent from the web-cam to filter pixels based on the hue of the reference object, and then find the 'centre of mass' of the largest object with the correct hue.²⁰ This was used to calculate the height of the interface between the reference points and control the speed of the light-phase-out pump *via* a serial interface. Due to the well documented serial communication protocol available,²¹ we opted to use two New-Era syringe pumps²² working as a dual-piston push–pull pair as the light-phase-out pump. In principle, any pump capable of receiving serial commands can be used. The feedback system, which was unoptimised, was able to keep the volume of the heavy phase in the separator steadily at 0.25 cm³ for long periods of time, affording minimal mixing/dispersion.²³ With the required machine components in hand, we chose as the initial reaction for study the simple condensation of benzaldehyde **1a** with phenylhydrazine **2** to form the hydrazone **3a**, using excess hydrazine with the aldehyde as the limiting reagent. Pyridinium toluenesulfonate (PPTS, 2 mol%) was also used as a catalyst. Aqueous 1 M phosphoric acid was used to extract the excess hydrazine. The flow setup used is shown in Fig. 2. The aldehyde–PPTS and hydrazine solutions were delivered *via* loading loops into two streams of DCM which meet at a t-piece.

Using a higher volume loop for the hydrazine, and injecting this slightly ahead of the aldehyde, ensured that the limiting aldehyde component was never present in the reaction loop without excess hydrazine also being present. The flow rate and

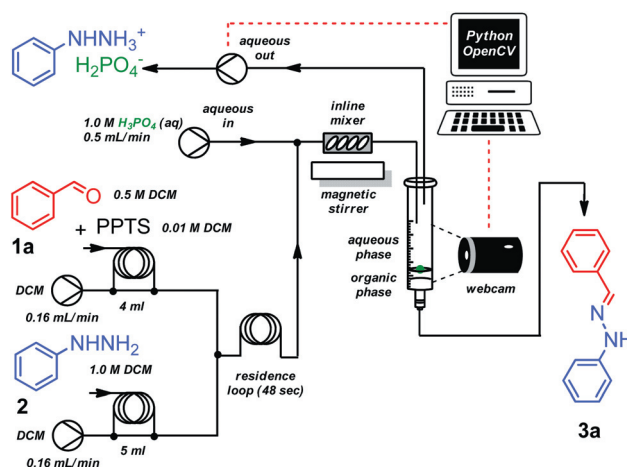


Fig. 2 Flow setup used for hydrazone formations.

volume of the residence loop were sufficient to give complete conversion (in 48 s). For several substrates, some turbidity was apparent in the reaction stream at the concentrations used. By using tubing/connectors with internal cross sections of 1 mm, blocking was avoided. The product stream meets the aqueous phosphoric acid stream at a t-piece and passes into the mixer, the output of which is fed into the separator vessel and the heavy DCM phase is collected. The product was recovered in quantitative yield simply by removing the solvent under reduced pressure. $^1\text{H}/^{13}\text{C}$ NMR spectra revealed the product to be analytically pure. These conditions were used for the formation of a series of hydrazones (Table 1), all with complete conversion and formed in practically quantitative yield. The system was then applied to a second reaction, the epoxidation of a series of allylic alcohols with excess *m*-CPBA. The excess *m*-CPBA and its by-product were extracted with an aqueous solution of sodium thiosulfate and sodium bicarbonate. A residence time of 10 min was required to give complete conversion. Again, product isolation was achieved simply by removal of solvent under reduced pressure and all the epoxides prepared were analytically pure and were isolated in practically quantitative yield (Table 2).

As a further example of the application of this new separator, the BF_3 promoted formation of dithianes from aldehydes and 1,3-propane dithiol (excess) was carried out (Table 3).

The aldehyde stream and the propane-dithiol- BF_3 stream were allowed to react for 60 s, before mixing with a stream of aqueous sodium hydroxide to quench the reaction and extract the excess dithiol. That the dithiol had been efficiently extracted from the product stream was apparent from the lack of odour associated with the compound. $^1\text{H}/^{13}\text{C}$ analysis also revealed that the products were indeed analytically pure. During these reactions, the presence of product in the outlet was monitored *qualitatively* by TLC. However, we sought to obtain a *quantitative* picture of the relationship between the volume of the heavy-phase in the separation vessel and the nature of the dispersion. To observe and record dispersion caused by mixing in the separation vessel, we used a dilute solution of the red dye Sudan IV in DCM, and a cheap USB-‘microscope’ to monitor the intensity of colour in the outlet tubing (Fig. 3).

There are several methods to calculate colour intensity from data in image files, depending on the file format. The approach we took was to calculate the proportion of total red channel values in the red, green and blue channels of RGB images

Table 1 Results of continuous flow hydrazone formation

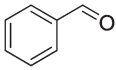
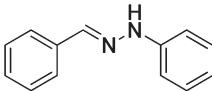
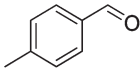
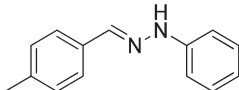
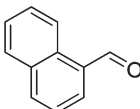
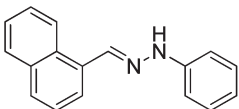
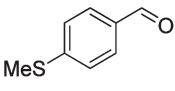
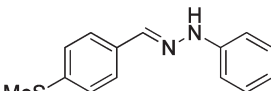
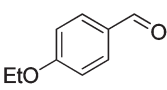
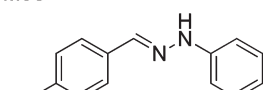
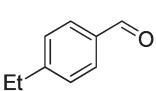
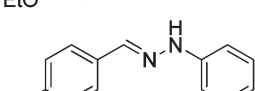
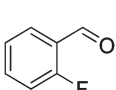
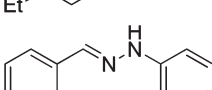
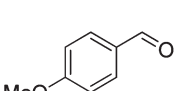
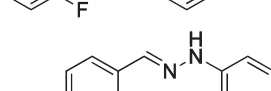
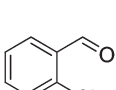
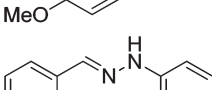
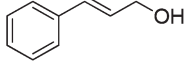
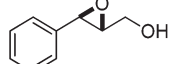
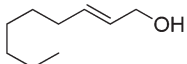
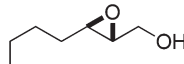
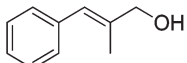
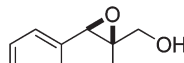
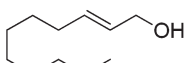
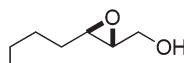
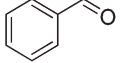
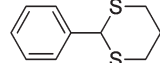
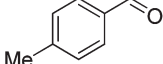
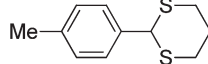
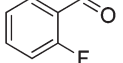
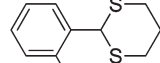
Entry	Substrate	Product	Yield
1			99
2			100
3			99
4			97
5			99
6			98
7			97
8			99
9			100

Table 2 Results of continuous flow epoxidation using excess *m*-CPBA^a

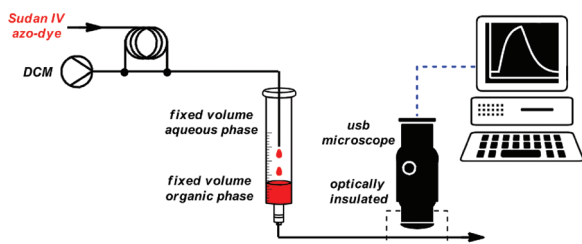
Entry	Substrate	Product	Yield
1			99
2			100
3			98
4			99

^a *m*-CPBA was purified by column chromatography on silica gel prior to use. Substrate injected as a 0.1 M solution in DCM *via* a 4 mL loop, flow rate 0.25 mL min⁻¹. *m*-CPBA 5, 0.4 M solution injected (30 s prior to substrate) *via* a 5 mL loop, flow rate 0.25 mL min⁻¹. Residence time for reaction: 10 min (5 mL loop). Quench solution of 0.5 M Na₂S₂O₃-NaHCO₃, flow rate 0.5 mL min⁻¹.

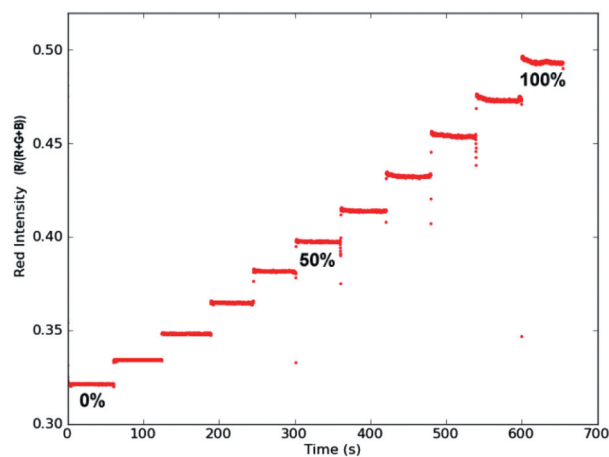
Table 3 Results of continuous flow dithiane formations^a

Entry	Substrate	Product	Yield
1			97
2			98
3			98

^a Substrate injected as 0.5 M solution in DCM *via* a 4 mL loop, flow rate 0.5 mL min⁻¹. Propane dithiol 8 (1.0 M) and BF₃·THF (0.75 M) injected (30 s prior to substrate) as a combined solution *via* a 5 mL loop, flow rate 0.5 mL min⁻¹. Residence time for reaction: 1 min (1 mL loop). Quench solution of 2 M NaOH, flow rate 0.5 mL min⁻¹.

**Fig. 3** Flow setup for dispersion measurements.

(in which each pixel has three values, for red (R), green (G) and blue (B) intensity respectively) of each video frame.²⁴ As shown in Fig. 4, the relationship between dye concentration and red colour intensity is approximately linear with a regression *R*² value of 0.998. The trace was obtained by injecting known dye concentrations into the observed tubing, in 10% concentration increments (of a 0.26 mM solution) every 60 s. Alternative approaches using HSV (Hue, Saturation, Value) image files were less fruitful. The camera assembly was isolated from ambient

**Fig. 4** Variation of 'red intensity' (R/(R+G+B)) with dye concentration.

light (that might affect readings) using aluminium foil. The same settings were used throughout. Shown in Fig. 5a are traces of the

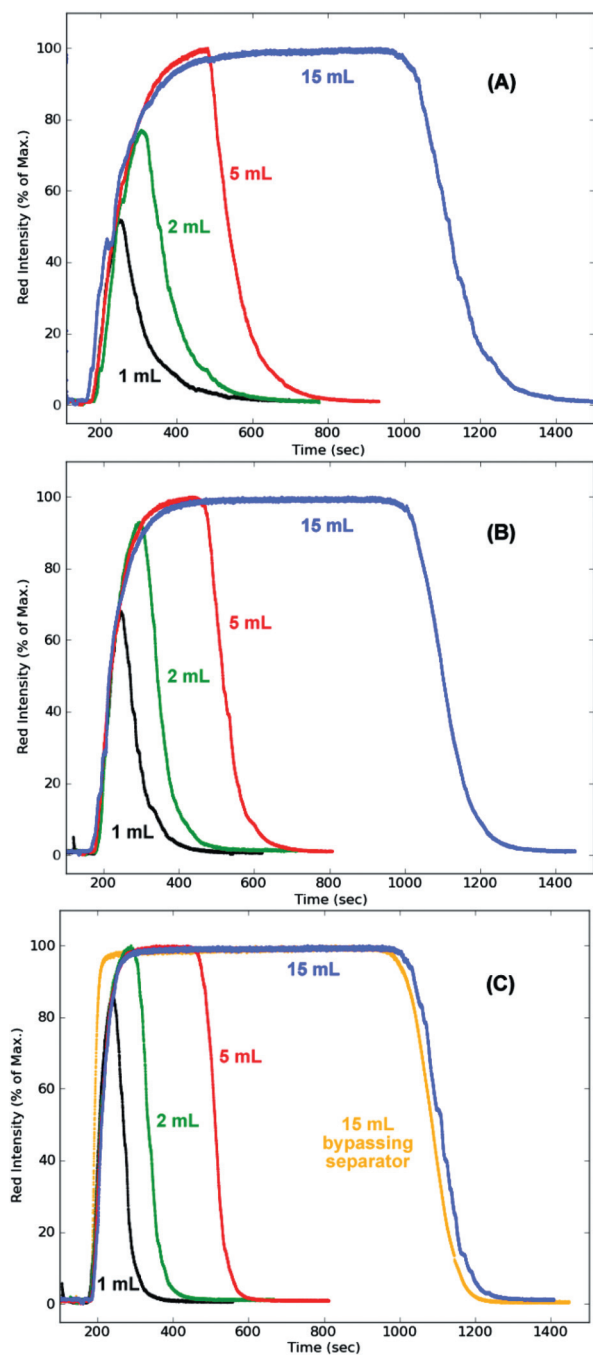


Fig. 5 Dispersion traces measured with a heavy phase volume of (a) 1 mL, (b) 0.5 mL and (c) 0.25 mL.

output colour intensity for a heavy-phase volume of 1 mL, with a series of injection loop volumes (1 mL min^{-1} flow rate). The slopes at the beginning and end of each recorded trace are the same for all injection volumes, as expected. Similar traces for 0.5 and 0.25 mL heavy-phase volumes are shown in Fig. 5b and 5c. With smaller heavy-phase volumes, the rise and decay slopes are steeper, *i.e.* less dispersion. With a 15 mL injection loop and a 0.25 mL heavy-phase volume, the observed intensity trace is almost identical to the trace from the control run bypassing the separator (orange trace Fig. 5c). The slope of the trailing edge of

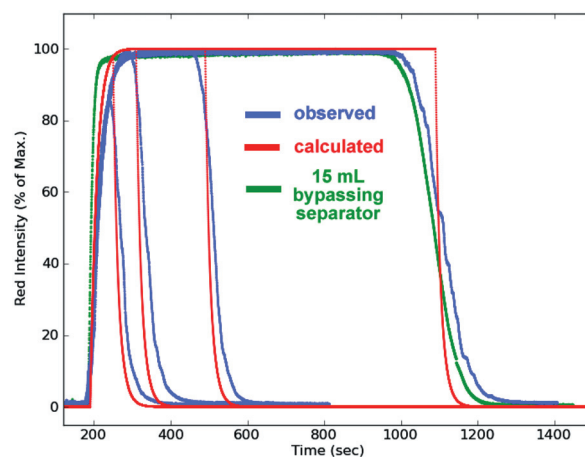


Fig. 6 Observed and calculated (well-stirred-tank) dispersion traces. Heavy phase volume of 0.25 mL, injection volumes of 1, 2, 5 and 15 mL, flow rate of 1 mL min^{-1} .

the control run (the output from the injection loop without the separator tank) is caused by axial dispersion within the tubing of the injection loop itself, the *dispersion caused by the separator is therefore negligible*. These traces show that, for a given injection volume, the output from the separator can be easily predicted with accuracy from previously recorded traces. It is also possible to model the dispersion mathematically. In the simplest ‘well-stirred-tank’ model,²⁵ the rise/decay functions are exponential. Fig. 6 shows the observed and calculated traces (for uniform ‘rectangular’ input injections) with a 0.25 cm^3 heavy-phase volume. To convert calculated concentrations to R/(R+G+B) intensities, a quartic polynomial was fitted to the calibration curve from Fig. 4, using a Vandermonde matrix interpolation. However, the difference between this and using the linear approximation, *i.e.* concentration (as % of max) \approx intensity (as % of max), was negligible. There is fairly good agreement between calculated and observed traces, especially at the start of the run. As can be seen from the control trace for the 15 mL loop in the absence of the separator altogether (green), the major difference at the trailing edges is actually due to dispersion inherent to the injection loops themselves, which could be modelled with a more detailed mathematical analysis and/or measured for any given injection loop.

The mixer used in this study, which was not optimised to minimise volume, will also provide some degree of dispersion (which we did not measure) and we are currently investigating the use of low-volume low-dispersion mixers.

In conclusion, this proof-of-concept study establishes the operation of a novel general-purpose system for continuous flow liquid–liquid extraction which uses a ‘computer-vision’ based approach to dynamic flow control. It was used successfully for hydrazone formations, alkene-epoxidations and dithiane syntheses, where the excess reagent was efficiently extracted into an aqueous stream to afford complete conversion to pure products that were isolated in very high yield simply by removal of solvent under reduced pressure. In addition to equipment that is commonplace in research laboratories, the system uses relatively cheap and readily available technology along with open-source software libraries so that the technique could easily be

implemented in any typical laboratory with a minimum of technical ability (see ESI†).

Notes and references

- For reviews and selected examples see: (a) J. Wegner, S. Ceylan and A. Kirschning, *Adv. Synth. Catal.*, 2012, **354**, 17–57; (b) C. Wiles and P. Watts, *Chem. Commun.*, 2011, **47**, 6512–6535; (c) D. Webb and T. F. Jamison, *Chem. Sci.*, 2010, **1**, 675–680; (d) J. I. Yoshida, *Chem. Rec.*, 2010, **10**, 332–341; (e) I. R. Baxendale, J. J. Hayward, S. Lanners, S. V. Ley and C. D. Smith, *Microreactors in Organic Synthesis and Catalysis*, ed. T. Wirth, Wiley, New York, 2008; (f) T. Razaq and C. O. Kappe, *Chem.–Asian J.*, 2010, **5**, 1274–1289; (g) B. Ahmed-Omer, J. C. Brandt and T. Wirth, *Org. Biomol. Chem.*, 2007, **5**, 733–740; (h) V. Hessel, *Chem. Eng. Technol.*, 2009, **32**, 1655–1681; (i) X. Y. Mak, P. Laurino and P. H. Seeberger, *Beilstein J. Org. Chem.*, 2009, **5**; (j) M. Brasholz, B. A. Johnson, J. M. Macdonald, A. Polyzos, J. Tsanaktisidis, S. Saubern, A. B. Holmes and J. H. Ryan, *Tetrahedron*, 2010, **66**, 6445–6449; (k) B. D. A. Hook, W. Dohle, P. R. Hirst, M. Pickworth, M. B. Berry and K. I. Booker-Milburn, *J. Org. Chem.*, 2005, **70**, 7558–7564; (l) A. R. Bogdan, S. L. Poe, D. C. Kubis, S. J. Broadwater and D. T. McQuade, *Angew. Chem., Int. Ed.*, 2009, **48**, 8547–8550; (m) R. L. Hartman, J. P. McMullen and K. E. Jensen, *Angew. Chem., Int. Ed.*, 2011, **50**, 7502–7519.
- S. V. Ley, I. R. Baxendale, R. N. Bream, P. S. Jackson, A. G. Leach, D. A. Longbottom, M. Nesi, J. S. Scott, R. I. Storer and S. J. Taylor, *J. Chem. Soc., Perkin Trans. 1*, 2000, 3815–4195.
- M. O'Brien, R. Denton and S. V. Ley, *Synthesis*, 2011, 1157–1192.
- E.g. at the time of writing, Sigma-Aldrich: Amberlite IRA 900 NaCO₃[−] form (540293) costs 82p (GB)/mmol. Standard Na₂CO₃·H₂O (S4132) costs 0.5p (GB)/mmol.
- For recent examples see: (a) X. C. Cambeiro, R. Martin-Rapun, P. O. Miranda, S. Sayalero, E. Alza, P. Llanes and M. A. Pericas, *Beilstein J. Org. Chem.*, 2011, **7**, 1486–1493; (b) C. Ayats, A. H. Henseler and M. A. Pericas, *ChemSusChem*, 2012, **5**, 320–325; (c) O. Bortolini, L. Cacioli, A. Cavazzini, V. Costa, R. Greco, A. Massi and L. Pasti, *Green Chem.*, 2012, **14**, 992–1000; (d) S. B. Otvos, I. M. Mandity and F. Fulop, *ChemSusChem*, 2012, **5**, 266–269; (e) M. O'Brien, N. Taylor, A. Polyzos, I. R. Baxendale and S. V. Ley, *Chem. Sci.*, 2011, **2**, 1250–1257.
- R. K. Sinnott and G. Towler, *Chemical Engineering Design*, Butterworth-Heinemann/Elsevier, Oxford, 2009.
- (a) J. G. Kralj, H. R. Sahoo and K. F. Jensen, *Lab Chip*, 2007, **7**, 256–263; (b) R. H. Atallah, J. Ruzicka and G. D. Christian, *Anal. Chem.*, 1987, **59**, 2909–2914; (c) O. K. Castell, C. J. Allender and D. A. Barrow, *Lab Chip*, 2009, **9**, 388–396; (d) E. Kolehmainen and I. Turunen, *Chem. Eng. Process.*, 2007, **46**, 834–839; (e) C. H. Hornung, M. R. Mackley, I. R. Baxendale and S. V. Ley, *Org. Process Res. Dev.*, 2007, **11**, 399–405; (f) H. R. Sahoo, J. G. Kralj and K. F. Jensen, *Angew. Chem., Int. Ed.*, 2007, **46**, 5704–5708.
- (a) E. Perperi, Y. L. Huang, P. Angeli, G. Manos and D. J. Cole-Hamilton, *J. Mol. Catal. A: Chem.*, 2004, **221**, 19–27; (b) E. L. Teo, G. K. Chuah, A. R. J. Huguet, S. Jaenicke, G. Pande and Y. Z. Zhu, *Catal. Today*, 2004, **97**, 263–270; (c) A. Yoshida, X. Hao and J. Nishikido, *Green Chem.*, 2003, **5**, 554–557; (d) J. F. B. Hall, X. Han, M. Poliakoff, R. A. Bourne and M. W. George, *Chem. Commun.*, 2012, **48**, 3073–3075.
- (a) R. P. Siraganian, *Anal. Biochem.*, 1974, **57**, 383–394; (b) S. L. Lin and H. P. Hwang, *Talanta*, 1993, **40**, 1077–1083; (c) N. Maleki, B. Haghighi and A. Safavi, *Microchem. J.*, 1996, **53**, 147–151; (d) K. Benz, K. P. Jäckel, K. J. Regenauer, J. Schiewe, K. Drese, W. Ehrfeld, V. Hessel and H. Löwe, *Chem. Eng. Technol.*, 2001, **24**, 11–17; (e) H. Sprecher, M. Payán, M. Weber, G. Yilmaz and G. Wille, *J. Flow. Chem.*, 2012, **2**, 20–23.
- H. Lange, C. F. Carter, M. D. Hopkin, A. Burke, J. G. Goode, I. R. Baxendale and S. V. Ley, *Chem. Sci.*, 2011, **2**, 765–769.
- R. E. Gugger and S. M. Mozersky, US 4054270, 1977.
- E. Maslana, R. Schmitt and J. Pan, *J. Autom. Methods Manage. Chem.*, 2000, **22**, 187–194.
- See ESI† for technical information including Python script.
- <http://www.python.org/> (last accessed 6/7/2012).
- <http://numpy.scipy.org/> (last accessed 6/7/2012).
- (a) <http://opencv.willowgarage.com/wiki/> (last accessed 6/7/2012); (b) G. Bradski, *Dr. Dobbs J.*, 2000, **25**, 120–125.
- <http://videocapture.sourceforge.net/> (last accessed 6/7/2012).
- <http://www.pythonware.com/products/pil/> (last accessed 6/7/2012).
- <http://pyserial.sourceforge.net/> (last accessed 6/7/2012).
- The following websites provided useful information and code examples: (a) <http://www.thisismyrobot.com/2010/05/object-tracking-in-opencv-and-python-26.html> (last accessed 6/7/2012); (b) <http://mikkeljans.blogspot.co.uk/2009/02/python-color-tracking.html> (last accessed 6/7/2012); (c) <http://www.davidhampgonsalves.com/2011/05/OpenCV-Python-Color-Based-Object-Tracking> (last accessed 6/7/2012).
- For another Python script that interfaces with New-Era syringe pumps see: <http://new-era-pump.readthedocs.org/en/latest/> (last accessed 6/7/2012).
- New Era Pump Systems, Inc., 138 Toledo Street, Farmingdale, NY 11735-6625 (pumps were supplied by the UK distributor: World Precision Instruments, 1 Hunting Gate, Hitchin, Hertfordshire, SG4 0TJ, UK).
- An approximately proportional control method was used in the code. The high and low pump speeds were capped, at 900 and 0.1 ml min^{−1} respectively, for operational reasons. Detailed quantitative investigations into the responsiveness of alternative control algorithms are ongoing and will be reported in due course.
- M. H. V. Werts, V. Raimbault, R. Texier-Picard, R. Poizat, O. Francais, L. Griscom and J. R. G. Navarro, *Lab Chip*, 2012, **12**, 808–820.
- (a) J. F. Tyson, *Anal. Chim. Acta*, 1986, **179**, 131–148; (b) J. F. Tyson, *Analyst*, 1990, **115**, 587–591; (c) E. A. G. Zagatto, J. M. T. Carneiro, S. Vicente, P. R. Fortes, J. L. M. Santos and J. Lima, *J. Anal. Chem.*, 2009, **64**, 524–532.